Energy Harvesting Multiple Access Channels: Optimal and Near-Optimal Online Policies

Abdulrahman Baknina, *Student Member, IEEE*, and Sennur Ulukus, *Fellow, IEEE*

***Abstract*— We consider *online* transmission policies for a two-user multiple access channel, where both users harvest energy from nature. The energy harvests are independent and identically distributed (i.i.d.) over time, but can be arbitrarily correlated between the two users. The transmitters are equipped with arbitrary but finite-sized batteries. We focus on the *online* case where the transmitters know the energy arrivals only causally as they happen. The users do not know the probability distribution of the energy arrivals; each user knows only its own average recharge rate. We consider the most general case of arbitrarily distributed energy arrivals with arbitrary correlation between the users. In order to study this general case, we first study a special case for the energy arrivals, namely, we first consider the special case of synchronized (i.e., fully-correlated) Bernoulli energy arrivals at the two users. Even though the energy arrivals are fully-correlated, average recharge rates at the users are different due to the different battery sizes. For this case, we determine the *exactly optimal* policies that achieve the boundary of the long-term average capacity region. We show that the optimal power allocation policy is decreasing within the renewal interval, and that the long-term average capacity region is a single pentagon. We then propose a distributed fractional power (DFP) policy, which users implement distributedly with no knowledge of the other user's energy arrival or battery state. We develop a lower bound on the performance of the DFP for synchronized Bernoulli energy arrivals. We then consider the case of two arbitrarily correlated asynchronous Bernoulli energy arrivals under the assumption of equal normalized average recharge rates. We show that extreme correlation between the energy sources hurts the achievable rate by showing that the throughput with asynchronous Bernoulli energy arrivals is larger than the throughput with the corresponding perfectly synchronized Bernoulli energy arrivals. We then show that under the DFP policy, the performance of Bernoulli energy arrivals forms a lower bound on the performance of any arbitrary energy arrivals. We also develop a universal upper bound on the performance of all online policies, and show that the proposed DFP is *near-optimal* in that it yields rates which are within a constant gap of the derived lower and upper bounds, and hence, of the optimal policy, for all system parameters.**

***Index Terms*— Energy harvesting communications, online scheduling, multiple access channel, power control, near-optimal policy, distributed policy.**

Manuscript received March 15, 2017; revised October 5, 2017 and December 22, 2017; accepted January 28, 2018. Date of publication February 6, 2018; date of current version July 13, 2018. This work was supported by NSF Grants CNS 13-14733, CCF 14-22111, CCF 14-22129, and CNS 15-26608. This paper was presented at the 2016 IEEE International Symposium on Information Theory, Barcelona, Spain, July 2016. The associate editor coordinating the review of this paper and approving it for publication was N. B. Mehta. *(Corresponding author: Sennur Ulukus.)*

The authors are with the Department of Electrical and Computer Engineering, University of Maryland, College Park, MD 20742 USA (e-mail: abaknina@umd.edu; ulukus@umd.edu).

Color versions of one or more of the figures in this paper are available online at http://ieeexplore.ieee.org.

Digital Object Identifier 10.1109/TCOMM.2018.2802918

I. Introduction

We consider a two-user energy harvesting multiple access channel, Fig. 1, where each user harvests energy from nature into its (arbitrary) finite-sized battery. The energy harvests at the transmitters are i.i.d. in time but can be arbitrarily correlated between the users at any instant. The average recharge rates[1] can be different, but we assume that average recharge rate per unit battery for both users is equal; each user knows only its own average recharge rate. We consider the *online* setting where the energy arrivals are known only causally at the transmitters. The users have no prior knowledge about the joint probability distribution of the energy harvesting processes. We study the *online* power scheduling problem where the users need to determine their transmit power levels based only on the energy arrival information so far. Our goal is to determine optimal and near-optimal online power allocation policies that achieve or approach the boundary of the long-term average capacity region. Here, by *near-optimal* policies, we mean policies which yield rates that are within a constant gap from the optimal policy for all system parameters.

Scheduling for energy harvesting systems has been considered in *offline* and *online* settings in recent research; see recent survey articles on scheduling approaches [1], [2]. When energy arrivals are known non-causally ahead of time, *offline* power allocation is studied, e.g., in [3]–[35], starting with the single-user setting in [3]–[6], generalizing to multi-user settings of broadcast, multiple access, cooperative multiple access and interference channels in [7]–[13] and relay and multi-hop settings in [14]–[18], incorporating non-ideal behavior at the transmitters including losses at the time of charging/discharging, energy leakage over time, processing costs and temperature increases [19]–[26]. Energy harvesting receivers are considered in [27]–[33], and energy cooperation and energy sharing concepts are studied in [34] and [35].

When energy arrivals are known only causally as they happen, *online* power allocation is studied, e.g., in [5], [6], and [36]-[56]. In this case, the transmitter needs to allocate its transmit power based on the causal knowledge of energy arrivals. For a transmitter with a finite-sized battery, using the available energy too slowly will result in wasting of the new incoming energy arrivals, while using it too fast will result in idling of the transmitter. In most cases, the online power control problem is formulated as a stochastic optimization problem, and Markov decision processes and dynamic programming approaches are used, and the solution is found

[1] In this paper, average recharge rate means average (expected value of) energy arrivals.

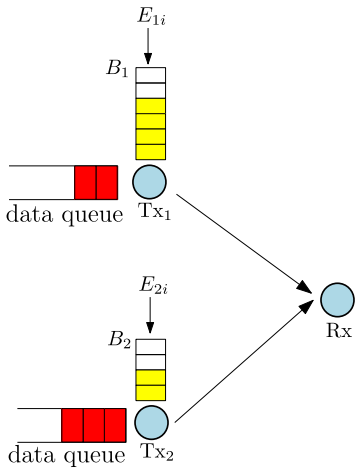

Fig. 1. System model: an energy harvesting multiple access channel model.

by solving Bellman equations [6], [36]–[41]. Low-complexity heuristic online algorithms are proposed in [5], [42], and [43]. In most of these works, either heuristic algorithms are proposed with no performance guarantees or optimal algorithms are proposed with no structural insights. Worst case performance guarantees when no statistical knowledge is available are studied in [44]–[47]. References [44] and [45] study the competitive ratio guarantees, and references [46] and [47] study Lyapunov techniques. In this paper, we assume the knowledge of the average recharge rate.

Our work in this paper is most closely related with [10] and [49]–[51]. Reference [10] develops optimum power allocation schemes for the energy harvesting multiple access channel in the offline setting using generalized directional water-filling techniques. References [49]–[51] develop a unique approach to the online power allocation problem in the single-user setting, by first considering a special Bernoulli energy arrival process which provides a *renewal* structure that enables analytical tractability, and then by generalizing it to general i.i.d. arrivals.[2] Recently, we have extended the approach in [49]–[51] to the case of broadcast channels [53], [54]. In this paper, we extend [49]–[51] to the case of multiple access channels. Going from the single-user channel to the multiple access channel brings up several challenges: in the multiple access channel the achievable rates are in a two-dimensional space; the powers of the users need to be optimized jointly; and the effect of the correlation between the energy arrivals at the two users need to be taken into acount. In the conference version of this paper [55], we focused on the case of fully-correlated energy arrivals, where the energy arrivals at the two users are synchronized; in this extended version of [55], we study the general version of the problem with arbitrarily correlated energy arrivals at both users. We acknowledge an independent and concurrent paper [56], which also considers the online power control problem for the multiple access channel.

While the end-results of our paper here and [56] are similar, there are differences in the scope and mathematical development of both papers. In this paper, we start with developing the exactly optimum power allocation scheme for the special case of fully-correlated Bernoulli energy arrivals, propose a distributed fractional power (DFP) policy inspired by the properties of the exactly optimum policy developed here, and then show that it is near-optimum for general energy arrivals under equal normalized recharge rates. In going from the fully-correlated to arbitrarily correlated Bernoulli energy arrivals, we show that Bernoulli energy arrivals with full correlation achieve long-term average rates no more than the long-term average rates achieved for any two arbitrarily correlated Bernoulli energy arrivals with the same mean. Hence, correlation between energy arrivals may decrease the maximum achievable long-term average rate. In contrast, [56] directly starts with a fractional policy inspired by the single-user solution, and shows that it is near-optimum by cleverly applying the results of the single-user channel in [49]–[51] for the most general case of energy arrivals.

In this paper, we consider the case of arbitrarily distributed energy arrivals with arbitrary correlation between the users and with equal normalized recharge rates at the users. We present the general system model in Section II. In order to study the general energy arrival case, we first study a special case for the energy arrivals. We first consider the case of fully-correlated Bernoulli energy arrivals in Section III. For this case, we obtain the jointly *optimum* online power schedules for the users. We show that, between the energy arrivals, the optimum transmission powers of both users decrease exponentially in time. We show that the long-term average capacity region, which is in general a union of pentagons, where each pentagon results from a different power allocation, is a single pentagon for fully-correlated Bernoulli energy arrivals. We show that at the corner points of the pentagon where one of the users gets the single-user rate, the user getting the single-user rate transmits for a shorter (or equal) duration than the other user.

Motivated by the fractional structure of the optimal policies for fully-correlated Bernoulli arrivals and the single pentagon structure of the long-term average capacity region, in Section IV, we propose a sub-optimal policy which is fixed but distributed between the users, coined *distributed fractional power* (DFP) policy. The DFP is *universal* in that, it does not depend on the distribution of the energy arrival processes; it depends only on the average recharge rate and the size of the battery at each user. Users implement this algorithm distributedly with no knowledge of the other user's energy arrival or battery state. We obtain a lower bound on the performance of the proposed DFP for the case of fully-correlated (synchronous) Bernoulli arrivals.

Next, in Section V, we study the general arbitrarily correlated energy arrivals. We first study arbitrarily correlated Bernoulli energy arrivals, in which case, the Bernoulli arrivals at the users are not synchronized. We show that under the DFP policy, the performance of the energy arrivals coming from a fully-correlated Bernoulli energy arrivals forms a lower bound on the performance of arbitrarily correlated Bernoulli energy arrivals with the same mean. Then, we show that the performance with Bernoulli energy arrivals forms a lower bound for the performance with any other energy arrivals with

[2]References [49], [52] make connections between information-theoretic capacity and optimal online power control.

the same mean. Finally, we derive a *universal* upper bound that is valid for all online policies. This upper bound is valid for general energy arrivals, and is universal in that it depends only on the average recharge rates at the users. We show that the derived upper and lower bounds are within a constant gap of each other, and hence, the proposed DFP policy achieves rates that are within a constant gap from the optimal online long-term average capacity region for the multiple access channel under equal normalized recharge rates.

Finally, in Section VI, we study the performance of the proposed DFP policy through several numerical results. We observe that the proposed DFP policy yields performance close to the performance of the optimal policy.

II. System Model

We consider a two-user energy harvesting multiple access channel. User k has a battery of size B_k, see Fig. 1. There are two energy harvesting sources which deliver $E_{ki} = e_{ki}$ amount of energy to the kth user in slot i; e_{ki} is a realization of the random variable E_{ki}. We assume that the slot duration is equal to unity. We assume without loss of generality that $E_{ki} \leq B_k$ almost surely. The energy harvests are i.i.d. in time but can be arbitrarily correlated between the users. The battery state of user k at time i, b_{ki}, evolves as $b_{k(i+1)} = \min\{B_k, b_{ki} - P_{ki} + e_{ki}\}$. Here, P_{ki} is the transmit power of user k at time i, which is limited as $P_{ki} \leq b_{ki}$.

The physical layer is a Gaussian multiple access channel with noise variance at the receiver equal to σ^2. The single slot capacity region, $\mathcal{C}(P_{1i}, P_{2i})$, of this channel in slot i is [57] (also see e.g., [10]):

$$r_{1i} \leq \frac{1}{2}\log\left(1+\frac{P_{1i}}{\sigma^2}\right) \tag{1}$$

$$r_{2i} \leq \frac{1}{2}\log\left(1+\frac{P_{2i}}{\sigma^2}\right) \tag{2}$$

$$r_{1i}+r_{2i} \leq \frac{1}{2}\log\left(1+\frac{P_{1i}+P_{2i}}{\sigma^2}\right) \tag{3}$$

The formulation here assumes that the slots are long enough that the coding is done within the course of each slot. This results in being able to achieve the capacity region in (1)-(3) in each slot i; see for example, [1]-[27], [32]-[35], [42], [43], and [49]-[57].

The above single slot capacity region is a pentagon. The overall capacity region is a union of all possible pentagons corresponding to all feasible power allocations over time, and thus, may no longer be a pentagon [10](see also [58]), as shown in Fig. 2. For a feasible policy at user k for n slots, we define a set of power allocations as: $P_k^n = [P_{k1}, \ldots, P_{kn}]$ where P_{ki} is a function of $(e_{ki}, e_{kj}, P_{kj}, b_{kj}, j \in \{1, \ldots, i-1\}, k \in \{1, 2\})$. Then, the n slot average achievable rate region under this policy is defined as:

$$r_1 \leq \mathbb{E}\left[\frac{1}{n}\sum_{i=1}^{n}\frac{1}{2}\log\left(1+\frac{P_{1i}}{\sigma^2}\right)\right] \tag{4}$$

$$r_2 \leq \mathbb{E}\left[\frac{1}{n}\sum_{i=1}^{n}\frac{1}{2}\log\left(1+\frac{P_{2i}}{\sigma^2}\right)\right] \tag{5}$$

$$r_1+r_2 \leq \mathbb{E}\left[\frac{1}{n}\sum_{i=1}^{n}\frac{1}{2}\log\left(1+\frac{P_{1i}+P_{2i}}{\sigma^2}\right)\right] \tag{6}$$

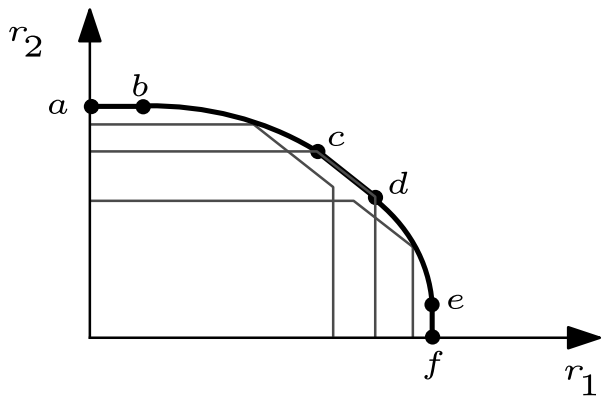

Fig. 2. Capacity region of a multiple access channel. Points a, f characterize the single-user rates, points c, d characterize the sum-rate and points b, e characterize the maximum rates achieved while the other user is operating with its single-user rate.

where the expectation is over the joint distribution of the energy arrivals. The long-term average capacity region is equal to the union of all such pentagons over all feasible policies as n tends to infinity. This is a convex region, see [10, Lemma 3].

We aim to characterize the long-term average rate region under online knowledge of the harvested energies. We first characterize the set of all feasible policies subject to causal knowledge of energy arrivals, denoted as $\hat{\mathcal{F}}$:

$$\hat{\mathcal{F}} = \{\forall i \in \{1,2,3,\ldots\}, \quad \forall k \in \{1,2\}, \\ P_{ki}(e_{ki}, e_{kj}, P_{kj}, b_{kj}, j \in \{1,\ldots,i-1\}, k \in \{1,2\}) | P_{ki} \leq b_{ki}\} \tag{7}$$

This defines the set of all admissible power policies. The power in each slot is constrained by the energy available in the battery and can be a function of all the previous power allocations, battery states, energy arrivals and the current energy arrival.

Since the long-term average rate region is convex, it can be characterized by its tangent lines; see [10], [58]. Therefore, the problem of characterizing the long-term average capacity region, which is the largest long-term average rate region, is equivalent to solving the following problem for all μ_1, $\mu_2 \in [0, 1]$,

$$\Phi = \sup_{P \in \hat{\mathcal{F}}} \lim_{n\to\infty} \mathbb{E}\left[\frac{1}{n}\sum_{i=1}^{n}(\mu_1 r_{1i} + \mu_2 r_{2i})\right] \tag{8}$$

where the rates (r_{1i}, r_{2i}) belongs to the capacity region in slot i, i.e., satisfies (1)-(3). The expectation is with respect to the joint distribution of the energy arrivals.

The stage reward in (8) is $(\mu_1\ r_{1i} + \mu_2\ r_{2i})$ and the admissible policies at each stage, $P_{1i} \times P_{2i}$, are the values in $[0, b_{1i}] \times [0, b_{2i}]$ which depend only on the current battery states b_{1i} and b_{2i}. Hence, an optimal policy exists and is Markovian, see e.g., [59, Th. 6.4] and [60, Th. 4.4.2]. We denote the rates achieved by an optimal Markovian policy for user j in slot i by r_{ji}^* and hence (8) can be rewritten as:

$$\Phi = \lim_{n\to\infty} \mathbb{E}\left[\frac{1}{n}\sum_{i=1}^{n}\left(\mu_1 r_{1i}^* + \mu_2 r_{2i}^*\right)\right] \tag{9}$$

The optimal Markovian policy can be found via dynamic programming by solving Bellman's equations [61, Ch. 4],

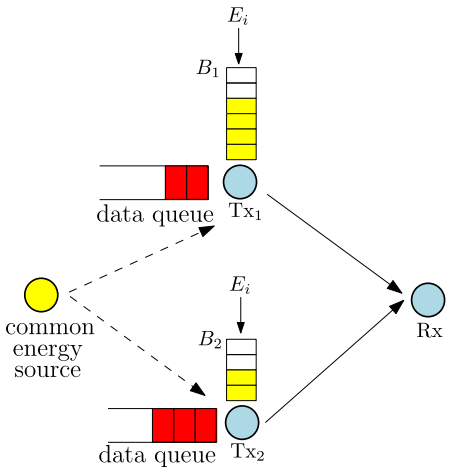

Fig. 3. System model: a synchronous energy harvesting multiple access channel model.

however, this will give little intuition or information about the structure of the solution. Instead, in the following, we develop a fixed and structured solution that will be exactly optimum for certain special energy arrivals and near-optimal for general energy arrivals.

We first study the special case of the fully-correlated (i.e., synchronized) Bernoulli energy arrivals with a particular support set in Section III, and determine the *exactly optimum* power allocation policies for this case. In this case, either no energy arrives, or when it arrives, it arrives simultaneously to both users, and it fills their respective batteries completely. That is, either $E_{1i} = E_{2i} = 0$ with probability $1-p$, or energies arrive in the amounts of $E_{1i} = B_1$ and $E_{2i} = B_2$ with probability p. Intuitively, we also coin this case as the *common energy source* case, see Fig. 3; see also [55]. In the common energy arrival analogy, there is a common energy source, where either $E_i \triangleq E_{1i} = E_{2i} = 0$ with probability $1-p$, or a common energy arrives in the amount of $E_i = B$ with probability p, where $B \geq \max\{B_1, B_2\}$. Such an energy arrival process implies that, when energy arrives, the batteries of both users fill completely. This constitutes a *renewal* for the system, and we can evaluate the optimal expected throughput analytically. In Section IV, we propose a distributed *near-optimal* power allocation policy and lower bound its performance under synchronous Bernoulli energy arrivals. By *near-optimal* policy, we mean a policy which yields rates that are within a constant gap from the optimal policy for all system parameters. In Section V, we show that under the near-optimal policy proposed in Section IV, the performance of asynchronous Bernoulli energy arrivals is lower bounded by the performance of synchronous Bernoulli energy arrivals with the same mean. We also show that the performance of the asynchronous Bernoulli energy arrivals forms a lower bound on the performance of all general energy arrivals.

III. Optimal Strategy: Case of Synchronous Bernoulli Energy Arrivals

For the synchronous case, see Fig. 3, the expectation in (8) is over a single random variable (the common energy arrival). Whenever a positive energy arrives, the battery states at both users are reset to the full battery state, i.e., we have $\mathbb{P}[E_{1i} = 0, E_{2i} = 0] = 1-p$ and $\mathbb{P}[E_{1i} = B_1, E_{2i} = B_2] = p$. Hence, whenever an energy arrives a *renewal* occurs. From [62, Th. 3.6.1], the long-term weighted average throughput is:

$$\lim_{n\to\infty} \mathbb{E}\left[\frac{1}{n}\sum_{i=1}^{n}\left(\mu_1\, r_{1i}^* + \mu_2\, r_{2i}^*\right)\right]$$

$$= \frac{1}{\mathbb{E}[L]}\mathbb{E}\left[\sum_{i=1}^{L}\left(\mu_1 r_{1i}^* + \mu_2 r_{2i}^*\right)\right] \tag{10}$$

$$= p\sum_{k=1}^{\infty} p(1-p)^{k-1}\sum_{i=1}^{k}\left(\mu_1 r_{1i}^* + \mu_2 r_{2i}^*\right) \tag{11}$$

$$= \sum_{i=1}^{\infty}\sum_{k=i}^{\infty} p^2(1-p)^{k-1}\left(\mu_1 r_{1i}^* + \mu_2 r_{2i}^*\right) \tag{12}$$

$$= \sum_{i=1}^{\infty} p(1-p)^{i-1}(\mu_1 r_{1i}^* + \mu_2 r_{2i}^*) \tag{13}$$

where L is the inter-energy arrival time which is geometric with parameter p, i.e., $\mathbb{E}[L] = \frac{1}{p}$.

Therefore, continuing from (13), we focus on the optimization problem:

$$\begin{aligned}\max_{\{P_{1i},P_{2i},r_{1i},r_{2i}\}} \quad & \sum_{i=1}^{\infty} p(1-p)^{i-1}\left(\mu_1\, r_{1i} + \mu_2\, r_{2i}\right)\\ \text{s.t.} \quad & (r_{1i}, r_{2i}) \in \mathcal{C}(P_{1i}, P_{2i}), \quad \forall i\\ & \sum_{i=1}^{\infty} P_{1i} \leq B_1\\ & \sum_{i=1}^{\infty} P_{2i} \leq B_2, \;\; P_{1i}, P_{2i} \geq 0, \quad \forall i\end{aligned} \tag{14}$$

This problem, in effect, maximizes the expected weighted sum rate until the next energy arrival, given that an energy arrival has just occurred. Point a in Fig. 2 represents the single-user rate for user 2, corresponding to $\mu_1 = 0$, and can be obtained as in [49] and [50]. Point b represents the largest rate user 1 gets when user 2 maintains its single-user rate; this point can be obtained by fixing the second user's rate at its single-user rate and maximizing the first user's rate. The line between points c and d represents the sum-rate line where the sum of the two users' rates is constant; these points are obtained by setting $\mu_1 = \mu_2$. The curved part of the long-term average capacity region between b and c is obtained by tracing μ_1, μ_2 over $\mu_1 < \mu_2$.

We first consider point a. At this point, $P_{1i} = 0$, and user 2 transmits with its optimum single-user rate [49], [50]:

$$P_{2i}^* = \frac{p(1-p)^{i-1}}{\lambda_2} - \sigma^2, \qquad i = 1, \ldots, \tilde{N}_2 \tag{15}$$

where the optimum power decreases in time and $\tilde{N}_2$ is the last slot where the power is positive; λ_2 in (15) is found by satisfying the total power constraint with equality.

Next, we consider point b. At this point, we maximize the first user's rate, after fixing the power allocation of the second

user to its optimal single-user power allocation P_{2i}^*:

$$\begin{aligned}\max_{\{P_{1i},r_{1i}\}} \quad & \sum_{i=1}^{\infty} p(1-p)^{i-1} r_{1i} \\ \text{s.t.} \quad & (r_{1i}, \mathcal{C}(P_{2i}^*)) \in \mathcal{C}(P_{1i}, P_{2i}^*) \\ & \sum_{i=1}^{\infty} P_{1i} \leq B_1, \;\; P_{1i} \geq 0, \quad \forall i \end{aligned} \tag{16}$$

where $C(P_{2i}^*) = \frac{1}{2}\log(1+P_{2i}^*)$ denotes the single-user capacity of user 2 with power P_{2i}^*; see point b in Fig. 2, see also [10], [58].

The Lagrangian of this problem is:

$$\begin{aligned}\mathcal{L} = -\sum_{i=1}^{\infty} p(1-p)^{i-1} \log\left(1+\frac{P_{1i}}{P_{2i}^*+\sigma^2}\right) \\ +\lambda_1\left(\sum_{i=1}^{\infty} P_{1i} - B_1\right) - \sum_{i=1}^{\infty} \nu_{1i} P_{1i} \end{aligned} \tag{17}$$

The KKT optimality conditions are:

$$P_{1i} = \frac{p(1-p)^{i-1}}{\lambda_1 - \nu_{1i}} - \sigma^2 - P_{2i}^* \tag{18}$$

along with complementary slackness and $\lambda_1, \nu_{1i} \geq 0$.

We prove that at point b user 1 transmits for a duration no shorter than user 2, before proceeding to determine P_{1i}^*.

Lemma 1: With synchronized i.i.d. Bernoulli energy arrivals, at point b, where user 2 gets its single-user capacity, user 1 transmits for a duration no shorter than user 2.

Proof: At point b in Fig. 2, the rate of user 2 is given by $\sum_{i=1}^{\infty} p(1-p)^{i-1}\log\left(1+\frac{P_{2i}}{\sigma^2}\right)$ and the optimal power allocation for user 2 is given by (15). The rate of user 1 at point b in Fig. 2 is given by $\sum_{i=1}^{\infty} p(1-p)^{i-1}\log\left(1+\frac{P_{1i}}{P_{2i}^*+\sigma^2}\right)$. The coefficient $p(1-p)^{i-1}$ in front of the ith term in this expression is decreasing in i. However, the interference term in the denominator, P_{2i}^*, is decreasing as well in i; see from (15). Therefore, for any power P_1 to be assigned to the first user: from the coefficient perspective, we should put this power at earlier i as the coefficient is higher there, however, from an interference perspective, we should put this power at later i as the interference is lower there. That is, there is a tension here between the pre-log coefficient and the interference in the denominator.

The rate achieved by user 1 will depend on the value of the interference caused by user 2. If user 1 transmits at slots $i = \{1,\ldots,\tilde{N}_2\}$, then from (15), by inserting P_{2i}^* into its rate expression, user 1 will achieve a rate equal to $p(1-p)^{i-1}\log\left(1+\frac{P_{1i}}{p(1-p)^{i-1}/\lambda_2}\right)$. On the other hand, if user 1 transmits at slots $i = \{\tilde{N}_2+1,\ldots\}$, it will achieve a rate equal to $p(1-p)^{i-1}\log\left(1+\frac{P_{1i}}{\sigma^2}\right)$; this follows as $P_{2i}^* = 0$ for slots $i = \{\tilde{N}_2+1,\ldots\}$.

We first consider the slots $i = \{1,\ldots,\tilde{N}_2\}$. We will show that if user 1 transmits in slots $i = \{1,\ldots,\tilde{N}_2\}$, it has to begin transmission at slot $i = 1$, i.e., it is sub-optimal for user 1 to have zero power in slot $i = 1$ while it puts a non-zero power at any of the slots $i = \{2,\ldots,\tilde{N}_2\}$. To see this, note that, the rate achieved in these slots can be written in the form $x\log\left(1+\frac{P_1\lambda_2}{x}\right)$, where we denoted $p(1-p)^{i-1}$ as x. The function $x\log\left(1+\frac{P_1\lambda_2}{x}\right)$ is increasing in x. Thus, if we have a single energy P_1 to put into this objective function, we will put it when x is larger, i.e., when i is smaller. This necessitates for user 1 to start as early as possible, i.e., at $i = 1$, instead of any other slot in $i = \{2,\ldots,\tilde{N}_2\}$.

We next consider the slots $i = \{\tilde{N}_2+1,\ldots\}$. We will show that if user 1 transmits in slots $i = \{\tilde{N}_2+1,\ldots\}$, it has to begin transmission at slot $i = \tilde{N}_2+1$, i.e., it is sub-optimal for user 1 to have zero power in slot $i = \tilde{N}_2+1$ while it puts a non-zero power at any of the slots $i = \{\tilde{N}_2+2,\ldots\}$. The objective function for $i > \tilde{N}_2$, is also decreasing in i and hence if we have a single energy P_1 to put into this objective function, we will put it in earlier slots, i.e., at $i = \tilde{N}_2+1$, instead of any other slot in $i = \{\tilde{N}_2+2,\ldots\}$.

We then consider slots $i = \tilde{N}_2$ and $\tilde{N}_2+1$. We will show that it is sub-optimal for user 1 to have zero power in slot $i = \tilde{N}_2$ while it puts non-zero power in slot $i = \tilde{N}_2+1$; hence, user 1 has to start its transmission at slot 1. To prove this, we show that the objective function also decreases from slot $\tilde{N}_2$ to slot $\tilde{N}_2+1$ as follows:

$$\begin{aligned} & p(1-p)^{\tilde{N}_2-1}\log\left(1+\frac{P_1}{p(1-p)^{\tilde{N}_2-1}/\lambda_2}\right) \\ & > p(1-p)^{\tilde{N}_2}\log\left(1+\frac{P_1}{p(1-p)^{\tilde{N}_2}/\lambda_2}\right) \\ & > p(1-p)^{\tilde{N}_2}\log\left(1+\frac{P_1}{\sigma^2}\right) \end{aligned}$$

where the last inequality follows since we have $\frac{p(1-p)^{\tilde{N}_2}}{\lambda_2} \leq \sigma^2$, as otherwise, P_{2i}^* would have been strictly greater than zero for $i = \tilde{N}_2+1$ as well from (15). Hence, user 1 starts its transmission in slot 1 and always utilizes earlier slots with the non-zero transmit power.

Then, the rest of the proof follows by contradiction. Assume user 1 has a transmission duration $\tilde{N}_1 < \tilde{N}_2$. Then,

$$\sum_{i=1}^{\tilde{N}_1}\left(\frac{1}{\lambda_1}-\frac{1}{\lambda_2}\right)p(1-p)^{i-1} = B_1 \tag{19}$$

Thus, we have $\frac{1}{\lambda_1}-\frac{1}{\lambda_2} > 0$. Next, by assumption, we have $P_{1i} = 0$, $P_{2i} > 0$ in slot $\tilde{N}_2$. Then, from (18), we have

$$P_{1\tilde{N}_2} = p(1-p)^{\tilde{N}_2-1}\left(\frac{1}{\lambda_1-\nu_{1\tilde{N}_2}}-\frac{1}{\lambda_2}\right) = 0 \tag{20}$$

However, since we have $\nu_{1\tilde{N}_2} \geq 0$ and $p(1-p)^{\tilde{N}_2-1} > 0$,

$$0 = \left(\frac{1}{\lambda_1-\nu_{1\tilde{N}_2}}-\frac{1}{\lambda_2}\right) \geq \left(\frac{1}{\lambda_1}-\frac{1}{\lambda_2}\right) > 0 \tag{21}$$

which is a contradiction. Thus, $\tilde{N}_1 \geq \tilde{N}_2$. ■

Hence, at point b, user 1 transmits for a duration $\tilde{N}_1$ where $\tilde{N}_1 \geq \tilde{N}_2$. At this point, user 2 transmits with its single-user

power allocation until $\tilde{N}_2$. Then, for user 1,

$$\sum_{i=1}^{\tilde{N}_2}\left(\frac{1}{\lambda_1}-\frac{1}{\lambda_2}\right)p(1-p)^{i-1}+\sum_{i=\tilde{N}_2+1}^{\tilde{N}_1}\left(\frac{p(1-p)^{i-1}}{\lambda_1}-\sigma^2\right)=B_1 \tag{22}$$

where λ_2 and $\tilde{N}_2$ are obtained from the second user's single-user power allocation, while λ_1 and $\tilde{N}_1$ are obtained from solving (22) and ensuring that the Lagrange multiplier λ_1 is non-negative, i.e., $\tilde{N}_1$ is the largest integer satisfying,

$$p(1-p)^{\tilde{N}_1-1}\geq\lambda_1\sigma^2 \tag{23}$$

and $\lambda_2>\lambda_1$, simultaneously. Solving (22) for λ_1 we have

$$\lambda_1=\frac{1-(1-p)^{\tilde{N}_1}}{B_1+(\tilde{N}_1-\tilde{N}_2)\sigma^2+\frac{1}{\lambda_2}(1-(1-p)^{\tilde{N}_2})} \tag{24}$$

Therefore, $\tilde{N}_1$ is the largest integer that satisfies (23) when λ_1 in (24) is inserted into (23).

We also note that, at point b, both users' powers are decreasing in time. It is clear that the second user's power is decreasing, as it follows the single-user allocation in (15). For user 1, it is clear from (22) that the power is decreasing for the first $\tilde{N}_2$ slots, and again decreasing from slot $\tilde{N}_2+1$ onwards. Thus, it remains to check the transition from slot $\tilde{N}_2$ to slot $\tilde{N}_2+1$. We have,

$$\begin{aligned}P_{1\tilde{N}_2}&=\left(\frac{1}{\lambda_1}-\frac{1}{\lambda_2}\right)p(1-p)^{\tilde{N}_2-1} &(25)\\ &\geq\left(\frac{1}{\lambda_1}-\frac{1}{\lambda_2}\right)p(1-p)^{\tilde{N}_2} &(26)\\ &\geq\frac{1}{\lambda_1}p(1-p)^{\tilde{N}_2}-\sigma^2 &(27)\\ &=P_{1(\tilde{N}_2+1)} &(28)\end{aligned}$$

where (26) follows since $(1-p)\leq 1$ and (28) follows since the second user's transmission ends at $\tilde{N}_2$, hence $\frac{p(1-p)^{\tilde{N}_2}}{\lambda_2}<\sigma^2$. Thus, the first user's power is also decreasing throughout its transmission. This concludes the characterization of the optimal policies achieving point b.

Next, we consider sum capacity achieving points between point c and point d. For the sum rate, problem (14) reduces to:

$$\begin{aligned}\max_{\{P_{1i},P_{2i}\}}\ &\frac{1}{2}\sum_{i=1}^{\infty}p(1-p)^{i-1}\log\left(1+\frac{P_{1i}+P_{2i}}{\sigma^2}\right)\\ \text{s.t.}\ &\sum_{i=1}^{\infty}P_{1i}\leq B_1\\ &\sum_{i=1}^{\infty}P_{2i}\leq B_2,\ \ P_{1i},P_{2i}\geq 0,\quad\forall i\end{aligned} \tag{29}$$

Consider the *relaxed* problem with a total power constraint:

$$\begin{aligned}\max_{\{P_{1i},P_{2i}\}}\ &\frac{1}{2}\sum_{i=1}^{\infty}p(1-p)^{i-1}\log\left(1+\frac{P_{1i}+P_{2i}}{\sigma^2}\right)\\ \text{s.t.}\ &\sum_{i=1}^{\infty}P_{1i}+P_{2i}\leq B_1+B_2,\ \ P_{1i},P_{2i}\geq 0,\quad\forall i\end{aligned} \tag{30}$$

First, we remark that problems in (29) and (30) are equivalent: This follows since, any optimal solution of (29) is also feasible in (30) with the same optimum value; and, any optimal solution for (30), $P_{1i}^*+P_{2i}^*$, can be made feasible in (29) by defining $P_{1i}=(P_{1i}^*+P_{2i}^*)\frac{B_1}{B_1+B_2}$ and $P_{2i}=(P_{1i}^*+P_{2i}^*)\frac{B_2}{B_1+B_2}$, with the same optimum value. The equivalence here is in the sense of [63].

Using this equivalence, we can find the sum-rate optimal policies by first solving a single-user problem with a battery size $B_s=B_1+B_2$, and then dividing the total power to users in a feasible way. The feasible policy is not unique, and each feasible policy results in a different point on the c-d line.

Next, we characterize the two extreme points of this line: c and d. From the single-user analysis in [49] and [50], it follows that the transmission duration $\tilde{N}$ is an increasing function of the battery size, i.e., the larger the battery, the longer the transmission duration will be, see also [54, Lemma 1]. Hence, in the optimal solution for (30), $P_{1i}^*+P_{2i}^*$ is positive for a duration $\tilde{N}_s$ which is no less than the durations for the single-user solutions of the users.

We now show that the extreme achievable sum rate optimal point c is actually the point b, i.e., the long-term average capacity region for the case of synchronized Bernoulli arrivals is a single pentagon. We will show this by showing that, given the optimum total power allocation policy in (30), a feasible distribution can be found such that the single-user capacity for either of the users (we will show for user 2) is achieved. We denote the optimal Lagrange multiplier and the transmission duration for problem (30) by λ_s and $\tilde{N}_s$, respectively. Similarly, we have λ_2 and $\tilde{N}_2$ for the second user single-user power allocation. It is sufficient to show that $\lambda_s\leq\lambda_2$, since it will imply:

$$\left(\frac{p(1-p)^{i-1}}{\lambda_s}-\sigma^2\right)-\left(\frac{p(1-p)^{i-1}}{\lambda_2}-\sigma^2\right)\geq 0 \tag{31}$$

Recall that we have $\tilde{N}_s\geq\tilde{N}_2$. First, if $\tilde{N}_s=\tilde{N}_2$, then we have

$$\begin{aligned}\sum_{i=1}^{\tilde{N}_2}\left(\frac{p(1-p)^{i-1}}{\lambda_2}-\sigma^2\right)&=B_2\leq B_1+B_2\\ &=\sum_{i=1}^{\tilde{N}_s}\left(\frac{p(1-p)^{i-1}}{\lambda_s}-\sigma^2\right)\end{aligned} \tag{32}$$

which can happen if and only if $\lambda_s\leq\lambda_2$. Next, if $\tilde{N}_s>\tilde{N}_2$, i.e., $\tilde{N}_s-1\geq\tilde{N}_2$, then we have,

$$\lambda_s\sigma^2\leq p(1-p)^{\tilde{N}_s-1}\leq p(1-p)^{\tilde{N}_2}<\lambda_2\sigma^2 \tag{33}$$

implying $\lambda_s<\lambda_2$. In (33) the middle inequality follows from the monotonicity, and the outer inequalities follow since $\lambda_s,\lambda_2,\tilde{N}_s,\tilde{N}_2$ satisfy their optimality conditions. Hence, we have proved the following result.

Lemma 2: With synchronized i.i.d. Bernoulli energy arrivals, the online long-term average capacity region of the multiple access channel is a single pentagon.

IV. Near-Optimal Strategy: Case of Synchronous General Energy Arrivals

In this section, we consider the general but synchronized i.i.d. energy arrivals, i.e., energy arrivals which are fully-correlated but not necessarily Bernoulli distributed. This can be represented by an arbitrary i.i.d. random variable $\beta_i \in [0,1]$ and then we have $E_{1i} = \beta_i B_1$, and $E_{2i} = \beta_i B_2$. Hence, there is only one source of randomness, which is the random variable β_i. We propose a sub-optimal online policy for this case, and develop a lower bound on its performance. Let the average recharge rate at user k be $\bar{P}_k$, where $\bar{P}_k = \lim_{n\to\infty} \frac{1}{n}\sum_{i=1}^{n} E_{ki} = \mathbb{E}[E_{ki}]$.

A. Distributed Fractional Power (DFP) Policy

We first define the proposed sub-optimal online policy, which we coin as distributed fractional power (DFP) policy, for Bernoulli arrivals and then generalize it to arbitrary arrivals. The optimal powers achieving any point on the capacity of the multiple access channel are exponentially decreasing, hence as in [49] and [50], this motivates us for a fractional structure for the sub-optimal policy. Moreover, the long-term average capacity region for Bernoulli arrivals is a single pentagon, this motivates that the policy need not depend on μ_1, μ_2. For Bernoulli arrivals, each transmitter transmits a fraction p of its available energy. The first user transmits with power $B_1\ p(1-p)^{i-1}$ and the second user transmits with power $B_2\ p(1-p)^{i-1}$ in slot i. In general, user k transmits with a fraction of $q_k \triangleq \frac{\bar{P}_k}{B_k}$ of its available energy in its battery, i.e., $P_{ki} = q_k b_{ki}$.

B. A Lower Bound on the Proposed Online Policy

Theorem 1: Under the proposed DFP policy, the achievable long-term average rate region with i.i.d. synchronous Bernoulli energy arrivals is lower bounded as,

$$r_1 \geq \frac{1}{2}\log\left(1+\frac{\bar{P}_1}{\sigma^2}\right) - 0.72 \tag{34}$$

$$r_2 \geq \frac{1}{2}\log\left(1+\frac{\bar{P}_2}{\sigma^2}\right) - 0.72 \tag{35}$$

$$r_1 + r_2 \geq \frac{1}{2}\log\left(1+\frac{\bar{P}_1+\bar{P}_2}{\sigma^2}\right) - 0.72 \tag{36}$$

Proof: It is clear that the achievable long-term average rate region with the proposed DFP is a pentagon, as it is a single policy which does not depend on μ_1, μ_2. Hence, the whole long-term average region is completely characterized by four points, which are shown by a, b, c, d in Fig. 4. Therefore, to lower bound this region it suffices to lower bound the points a, b, c and d. Points a and d are the single-user rates which can be lower bounded as in [50] to obtain $r_1 \geq \frac{1}{2}\log\left(1+\frac{\bar{P}_1}{\sigma^2}\right) - 0.72$ and $r_2 \geq \frac{1}{2}\log\left(1+\frac{\bar{P}_2}{\sigma^2}\right) - 0.72$, which are (34) and (35), respectively. These identify points a', d'. Then, we lower bound the achievable sum rate by noting for the proposed policy: $P_{1i}+P_{2i} = (B_1+B_2)p(1-p)^{i-1}$. Hence, again using [50], we have (36). This identifies points b', c'. ■

Since the long-term average rate region with the DFP policy is a pentagon even for general energy arrivals, to show that Bernoulli arrivals give a lower bound for all other energy arrivals, it suffices to show it only for the single-user and sum rates. These follow directly for the single-user rates from [50, Proposition 4]. It also follows for the sum rate, since the expectation is taken over a single random variable which is the fully-correlated energy arrival process. Hence, [50, Lemma 2] can still be applied and the proof follows similar to the proof of [50, Proposition 4].

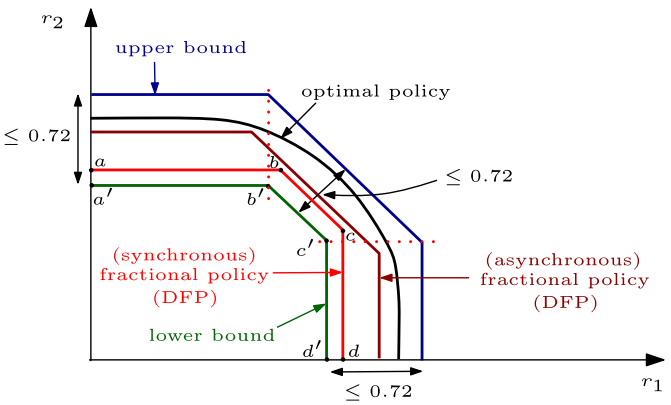

Fig. 4. Relationships between the bounds. We compare: universal lower bound, DFP policy for fully-correlated energy arrivals, DFP policy for arbitrary-correlated energy arrivals, optimal policy and a univeral upper bound.

Theorem 2: With the DFP policy, any arbitrary i.i.d. synchronous energy arrival process yields an achievable long-term average rate region no smaller than the long-term average rate region an i.i.d. synchronous Bernoulli energy arrival process with the same recharge rate yields.

V. General Energy Arrivals

In this section, we study the case of general i.i.d. energy arrivals. We first study the relation between synchronous and asynchronous Bernoulli energy arrivals. We show that under the DFP policy and i.i.d. Bernoulli energy arrivals, the performance of synchronous Bernoulli energy arrivals forms a lower bound for the performance of all asynchronous Bernoulli energy arrivals with the same mean. We then show that under the DFP policy and i.i.d. energy arrivals, the performance of asynchronous Bernoulli energy arrivals forms a lower bound for the performance of all general energy arrivals with the same mean. Finally, we develop a universal upper bound for all online policies. We show that the gap between the developed upper bound and the performance of the DFP under i.i.d. synchronous Bernoulli energy arrivals is finite for all system parameters. This implies that the performance of the DFP policy for any general energy arrival process is within a constant gap from the performance of the optimal online policy for energy arrivals which have equal recharge rate per unit battery.

A. Relation Between Synchronous and Asynchronous Bernoulli Energy Arrivals

Consider a synchronous Bernoulli energy arrival process where $\mathbb{P}[E_{1i} = 0, E_{2i} = 0] = 1-p$ and $\mathbb{P}[E_{1i} = B_1, E_{2i} = B_2] = p$; we denote the expectation over this distribution by $\mathbb{E}_{sync}[\cdot]$. Now, consider any arbitrary asynchronous

Bernoulli energy arrival process where $\mathbb{P}[E_{1i}=0,E_{2i}=0]=p_{00}$, $\mathbb{P}[E_{1i}=0,E_{2i}=B_2]=p_{01}$, $\mathbb{P}[E_{1i}=B_1,E_{2i}=0]=p_{10}$ and $\mathbb{P}[E_{1i}=B_1,E_{2i}=B_2]=p_{11}$; we denote the expectation over this distribution by $\mathbb{E}_{async}[\cdot]$. For a fair comparison, we require that the marginal distributions of the users in the synchronous and asynchronous cases are the same. In fact, for Bernoulli arrivals, requiring the marginals to be the same is equivalent to requiring the average recharge rates to be the same. Under this condition, we need $p_{00}+p_{01}=p_{00}+p_{10}=1-p$ and $p_{11}+p_{01}=p_{11}+p_{10}=p$. This implies that $p_{01}=p_{10}$, i.e., the joint distribution is symmetric.

We will now show that, under the DFP policy, the achievable long-term average rate region with synchronous Bernoulli arrivals is smaller than the achievable long-term average rate region with asynchronous Bernoulli arrivals for all permissible probability distributions. We first note that both achievable long-term average regions are pentagons, therefore, we only need to investigate individual rates and the sum rates. We also note that the individual rates are identical in synchronous and asynchronous cases, as the marginal distributions are identical. Therefore, we only need to investigate the sum rates in both cases.

We will need the following lemma for this investigation. This lemma states that, due to the concavity of logarithm, extreme values for transmit power give lower objective functions (rates) than all other intermediate values. Intuitively, in the synchronous case, the battery levels of the two users are either high or low simultaneously, implying simultaneous high or low transmit powers, therefore, high or low sum powers inside the logarithm. On the other hand, in the asynchronous case, the users will have mixed battery states (one battery level high, other battery level low), implying that users' transmit powers will be disparate and balance each other out. This, in effect, will average out the power components inside the logarithm of the sum rate, and will yield larger sum rates for the asynchronous case.

Lemma 3: For any four non-negative numbers x,y,w,z, with $w\leq(x,y)\leq z$ and $x+y=w+z$, the following inequality holds,

$$\log(x)+\log(y)\geq\log(w)+\log(z) \tag{37}$$

Proof: Since we have $w\leq(x,y)\leq z$, we can write x as a convex combination of w,z, i.e., for some $\alpha\in[0,1]$

$$x=\alpha w+(1-\alpha)z \tag{38}$$

Then, inserting this in $x+y=w+z$, we have

$$y=(1-\alpha)w+\alpha z \tag{39}$$

From the concavity of the log function, we have

$$\begin{aligned}&\log(x)+\log(y)\\&\quad=\log(\alpha w+(1-\alpha)z)+\log((1-\alpha)w+\alpha z) &(40)\\&\quad\geq\alpha\log(w)+(1-\alpha)\log(z)+(1-\alpha)\log(w)+\alpha\log(z) &(41)\\&\quad=\log(w)+\log(z) &(42)\end{aligned}$$

completing the proof.

Alternatively, we note that the relationship between the vectors $[x,y]$ and $[w,z]$ is exactly that of majorization [64], i.e., the vector $[x,y]$ is majorized by the vector $[w,z]$. That is, the components of $[x,y]$ are more nearly equal than the components of $[w,z]$. As the function $\Theta(x,y)=\log(x)+\log(y)$ is Schur-concave, from [64, Proposition C.1], we have $\Theta(x,y)\geq\Theta(w,z)$, i.e., more nearly equal components through a concave function yield larger values. ■

We now show in the following theorem that the performance of DFP with asynchronous Bernoulli energy arrivals is lower bounded by the performance of DFP with synchronous Bernoulli energy arrivals (with the same individual recharge rates). This theorem implies that extreme correlation between energy arrivals at the users affects the achievable rates negatively.

Theorem 3: With the DFP policy, any arbitrarily correlated (i.e., asynchronous) i.i.d. Bernoulli energy arrival process yields an achievable long-term average rate region no smaller than the long-term average rate region a fully-correlated (i.e., synchronous) i.i.d. Bernoulli energy arrival process yields.

We provide the proof of Theorem 3 in the Appendix.

B. Non-Bernoulli Energy Arrivals

We now relate the performance of asynchronous i.i.d. Bernoulli energy arrivals and any general i.i.d. energy arrivals with the same mean. The energy arrivals belong to any arbitrary distribution, i.e., $E_{1i}\in[0,B_1]$ and $E_{2i}\in[0,B_2]$ with arbitrary correlation between them. We first state the following lemma which is an extension of [50, Lemma 2] to the case of two random variables. This lemma compares the expected value of a concave function over Bernoulli and non-Bernoulli random variables. While we state the lemma for jointly concave functions, in fact, individual concavity of the function with respect to each variable is sufficient for the proof. In our case, the function is the sum rate which is jointly concave with respect to both user powers.

Lemma 4: Let $f(x,y)$ be a jointly concave function in x,y on $[0,B_1]\times[0,B_2]$. Let X,Y be random variables arbitrarily distributed on $[0,B_1]\times[0,B_2]$. Let $(\hat{X},\hat{Y})$ be Bernoulli random variables distributed on the same support set with the probability mass function $p_{11}=\frac{\mathbb{E}[XY]}{B_1B_2}$, $p_{10}=\frac{\mathbb{E}[X]}{B_1}-\frac{\mathbb{E}[XY]}{B_1B_2}$, $p_{01}=\frac{\mathbb{E}[Y]}{B_2}-\frac{\mathbb{E}[XY]}{B_1B_2}$, and $p_{00}=1-\frac{\mathbb{E}[X]}{B_1}-\frac{\mathbb{E}[Y]}{B_2}+\frac{\mathbb{E}[XY]}{B_1B_2}$. Then,

$$\mathbb{E}[f(\hat{X},\hat{Y})]\leq\mathbb{E}[f(X,Y)] \tag{43}$$

Proof: Applying the concavity of $f(x,y)$ first with respect to x and then with respect to y,

$$\begin{aligned}f(x,y)&\geq\frac{x}{B_1}f(B_1,y)+\frac{B_1-x}{B_1}f(0,y) &(44)\\&\geq\frac{B_2-y}{B_2}\frac{x}{B_1}f(B_1,0)+\frac{y}{B_2}\frac{x}{B_1}f(B_1,B_2)\\&\quad+\frac{B_2-y}{B_2}\frac{B_1-x}{B_1}f(0,0)+\frac{y}{B_2}\frac{B_1-x}{B_1}f(0,B_2) &(45)\end{aligned}$$

Then, setting $x=X,y=Y$, taking the expectation of both sides, and applying the relationship between the probability

mass function of the Bernoulli random variable and the expectations as described above, gives the desired result. ■

The following theorem relates the performance of the DFP policy under Bernoulli and general energy arrivals. The proof follows similar to [50, Proposition 4] using Lemma 4 above.

Theorem 4: With the DFP policy, any general i.i.d. energy arrival process yields an achievable long-term average rate region no smaller than the long-term average rate region a corresponding arbitrary (i.e., asynchronous) i.i.d. Bernoulli energy arrival process with the same recharge rate yields.

C. An Upper Bound for Online Policies

We now develop an upper bound which is valid for all online policies. This upper bound is universal in that it does not depend on the joint distribution of the energy arrival processes. It is valid for all energy arrival processes, and depends only on the average recharge rates of the energy arrival processes.

Theorem 5: The online long-term average capacity region for the multiple access channel is upper bounded as,

$$r_1 \leq \frac{1}{2}\log\left(1+\frac{\bar{P}_1}{\sigma^2}\right) \tag{46}$$

$$r_2 \leq \frac{1}{2}\log\left(1+\frac{\bar{P}_2}{\sigma^2}\right) \tag{47}$$

$$r_1+r_2 \leq \frac{1}{2}\log\left(1+\frac{\bar{P}_1+\bar{P}_2}{\sigma^2}\right) \tag{48}$$

where $\bar{P}_k$ is the average recharge rate of user k.

Proof: The achievable long-term average rate region for any online policy is upper bounded by the achievable long-term average rate region with the optimum offline policy, where all of the energy arrival information is known non-causally ahead of time. In addition, the achievable long-term average rate region with finite-sized battery is upper bounded by the achievable long-term average rate region with an unlimited-sized battery. For the offline problem, eliminating the *no-energy-overflow* constraints due to the finite battery size, the feasible set for the transmit power policy for user k, denoted as g_k^n, becomes

$$\mathcal{F}_k^n \triangleq \left\{\{g_{ki}\}_{i=1}^n : \frac{1}{m}\sum_{i=1}^{m} g_{ki} \leq \frac{1}{m}\left(\sum_{i=1}^{m} E_{ki}+B_k\right), \quad m=1,\ldots,n\right\}, \quad k=1,2 \tag{49}$$

where we have added B_k to the right hand side of (49) to allow for the case when the system has started with a full battery at the beginning of the communication session. We assume without loss of generality that $E_{ki} \leq B_k$. Next, we define a larger feasible set as,

$$\mathcal{G}^n \triangleq \left\{\{g_{1i}\}_{i=1}^n, \{g_{2i}\}_{i=1}^n : \frac{1}{n}\sum_{i=1}^{n} g_{1i}+g_{2i} \leq \frac{1}{n}\left(\sum_{i=1}^{n} E_{1i}+B_1+\sum_{i=1}^{n} E_{2i}+B_2\right)\right\} \tag{50}$$

which is formed by considering only one of the constraints for $m=n$ instead of all of the constraints $m=1,\ldots,n$ in the set $\mathcal{F}_k^n$, and by adding up the inequalities. Then, the offline sum rate is upper bounded as,

$$R_{off} \triangleq \lim_{n\to\infty} \max_{\{g_{ki}\}_{i=1}^n \in \mathcal{F}_k^n} \frac{1}{n}\sum_{i=1}^{n}\frac{1}{2}\log\left(1+\frac{g_{1i}+g_{2i}}{\sigma^2}\right) \tag{51}$$

$$\leq \lim_{n\to\infty} \max_{\{g_{ki}\}_{i=1}^n \in \mathcal{G}^n} \frac{1}{n}\sum_{i=1}^{n}\frac{1}{2}\log\left(1+\frac{g_{1i}+g_{2i}}{\sigma^2}\right) \tag{52}$$

$$\leq \lim_{n\to\infty} \max_{\{g_{ki}\}_{i=1}^n \in \mathcal{G}^n} \frac{1}{2}\log\left(1+\frac{\frac{1}{n}\left(\sum_{i=1}^{n} g_{1i}+g_{2i}\right)}{\sigma^2}\right) \tag{53}$$

$$\leq \lim_{n\to\infty} \frac{1}{2}\log\left(1+\frac{\frac{1}{n}\left(\sum_{i=1}^{n} E_{1i}+B_1+\sum_{i=1}^{n} E_{2i}+B_2\right)}{\sigma^2}\right) \tag{54}$$

$$= \frac{1}{2}\log\left(1+\frac{\bar{P}_1+\bar{P}_2}{\sigma^2}\right) \tag{55}$$

where (52) follows because $\mathcal{G}^n$ is a larger feasible set, (53) follows from the concavity of the log function, (54) follows by applying the inequality in $\mathcal{G}^n$, and (55) follows by the strong law of large numbers and since the remaining $\frac{1}{n}B_k$ terms go to zero as n tends to infinity. This proves (48). The proofs for (46) and (47) follow similarly. ■

Finally, comparing the lower bound in Theorem 1 and the upper bound in Theorem 5, we note that the distance in all directions is bounded by a finite number (0.72 in this case) which is independent of all system parameters. We recall that: 1) the lower bound in Theorem 1 is valid for all synchronous Bernoulli arrivals; 2) by Theorem 2, the rates of any general synchronous energy arrivals are no smaller than the rates of synchronous Bernoulli arrivals; 3) by Theorem 3, the rates of any arbitrary (asynchronous) Bernoulli arrivals are no smaller than the rates of a corresponding synchronous Bernoulli arrivals; and 4) by Theorem 4, the rates of any arbitrary energy arrivals are no smaller than a corresponding arbitrary (asynchronous) Bernoulli arrivals.

To complete the argument, and put everything together, we note the following subtlety: Starting from any arbitrary energy arrival processes, the Bernoulli energy arrivals obtained in Theorem 4 (see the construction of the joint probability mass function in Lemma 4) is not in general such that $p_{01}=p_{10}$, which is required by Theorem 3. Note that, we have $p_{01}=p_{10}$, if the average recharge rates per unit battery are equal, i.e., $\frac{\bar{P}_1}{B_1}=\frac{\bar{P}_2}{B_2}$. This ensures $\frac{\mathbb{E}[X]}{B_1}=\frac{\mathbb{E}[Y]}{B_2}$ in Lemma 4, and therefore, ensures $p_{01}=p_{10}$. We refer to this condition as either *equal normalized recharge rates,* or alternatively as *equal recharge rates per unit battery.* Our final result therefore is that, under *equal recharge rates per unit battery*, the proposed DFP policy is near-optimal as it yields rates that are within a constant gap from the optimal online policy for all system parameters.

We note though that this restriction is not too strict as it does not necessarily imply a complete symmetry in the system with $B_1=B_2$ and $\bar{P}_1=\bar{P}_2$. For instance, all uniform distributed energy arrival processes with realizations in $[0, B_k]$ satisfy this condition. This restriction allows us to make a direct

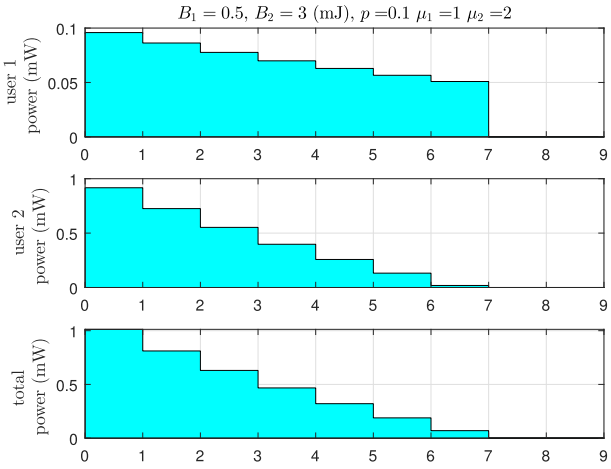

Fig. 5. Optimal powers for Bernoulli arrivals (fully-correlated arrivals).

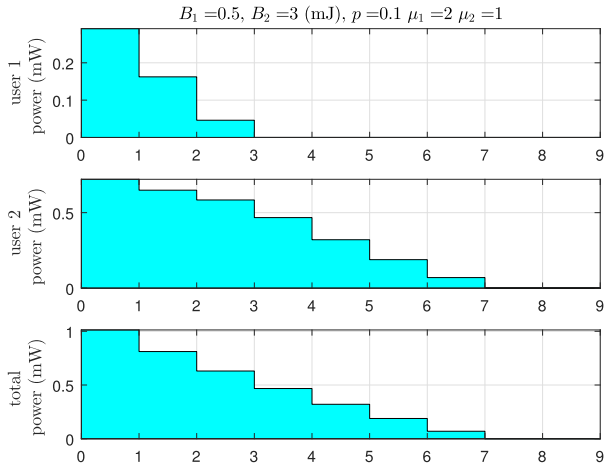

Fig. 6. Optimal powers for Bernoulli arrivals (fully-correlated arrivals).

comparison between synchronous and asynchronous Bernoulli energy arrivals as in Theorem 3, and gives more intuition. We note that the same lower bound follows without this condition as in [56] without making any comparisons with fully-synchronized energy arrivals.

We show the relationships between the bounds derived in this paper in Fig. 4.

VI. Numerical Examples

In this section, we illustrate the results obtained through several numerical examples. We set $\sigma^2 = 1$ mW (milli-Watt). We first consider the case of fully-correlated (synchronized) i.i.d. Bernoulli energy arrivals. For the corner point where user 2 operates at its single-user capacity, i.e., when $\mu_2 > \mu_1$, we plot the optimal power allocations in Fig. 5, for $p = 0.1$, $B_1 = 0.5$ mJ (milli-Joule) and $B_2 = 3$ mJ. As we proved, user 1 transmits for a longer duration than user 2, and user 2 follows its single-user power allocation. Note that this occurs even though the battery at user 1 is much smaller than the battery at user 2. Similarly, when $\mu_1 > \mu_2$, Fig. 6 shows that user 1 operates at its single-user rate and user 2 transmits for a longer duration. We then plot the total power achieving the

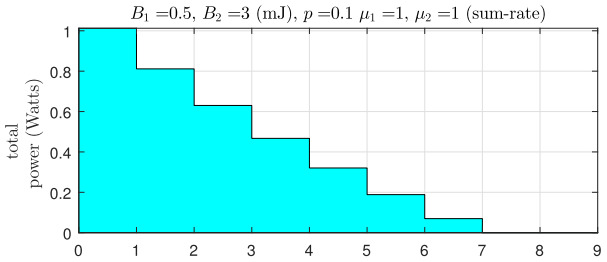

Fig. 7. Optimal powers for Bernoulli arrivals (fully-correlated arrivals).

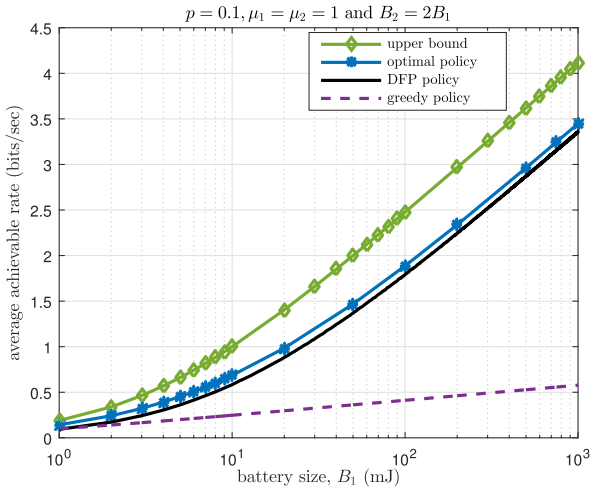

Fig. 8. Sum rate: optimal policy, DFP policy, greedy policy and upper bound (fully-correlated Bernoulli arrivals).

optimal long-term average sum-rate in Fig. 7. As we proved, the total power is higher than the optimal single-user power allocations of the users in every slot.

Next, we show the performance of the proposed DFP policy versus the optimal online policy and the upper bound in Fig. 8 for fully-correlated Bernoulli arrivals. We study the sum-rate point at which we have $\mu_1 = \mu_2$. We observe that DFP performs close to the optimal. We also study the performance of the greedy policy in which the transmitter transmits whenever there is energy in the battery. We notice that the performance of the greedy policy is poor. The reason for this poor performance is that under Bernoulli arrivals, the transmitters transmits with probability p a rate of $\frac{1}{2}\log(1 + B_1 + B_2)$ and remains silent with probability $1 - p$, thus, the long-term average throughput is equal to $p\frac{1}{2}\log(1 + B_1 + B_2)$ and for low values of p this rate is far from optimal.

In Fig. 9, we study the performance of the DFP policy for the fully-correlated Bernoulli energy arrivals under fixed average recharge rate. We fix the average recharge rate to $\bar{P}_1 = 1$mJ and $\bar{P}_2 = 2$mJ. The performance of the DFP policy is close to the performance of the optimal policy. The performance of both the optimal and the DFP policies decrease with the battery size. This is because the average recharge rate for the Bernoulli arrivals is equal to $\bar{P}_k = B_k p$, thus, for a fixed average recharge rate, as the value of the battery increases the value of p decreases. The smaller the value of p the less frequent the energy will arrive and this will degrade the performance.

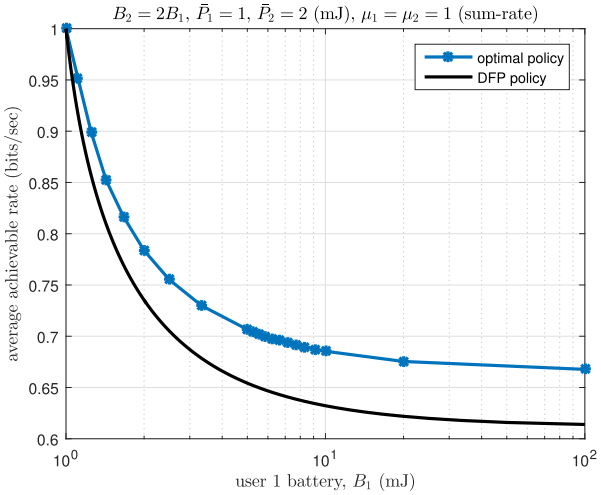

Fig. 9. Sum rate: optimal policy and DFP policy (fully-correlated Bernoulli arrivals) for fixed average recharge rate.

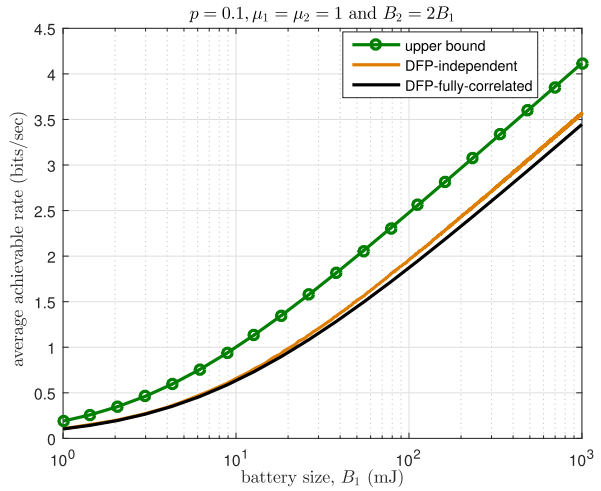

Fig. 10. Sum rate: Upper bound and DFP policy (fully-correlated and independent Bernoulli arrivals).

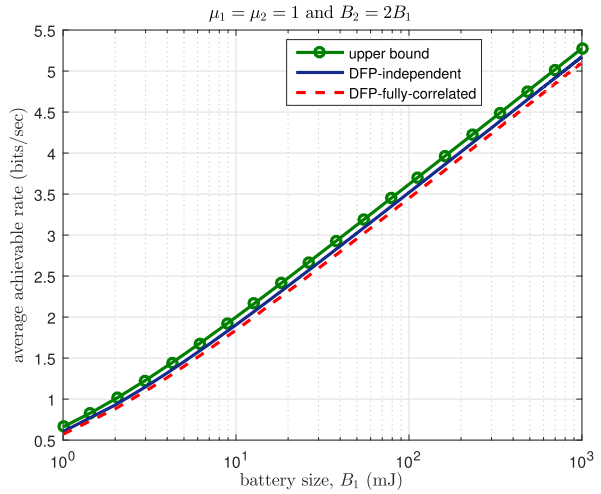

Fig. 11. Sum rate: Upper bound and DFP policy (fully-correlated and independent uniform arrivals).

In Fig. 10, we compare the performance of the DFP policy for fully-correlated and independent Bernoulli energy arrivals. As proved, the achievable performance of fully-correlated energy arrivals serves as a lower bound for the performance of asynchronous (in this case completely independent) energy arrivals. In Fig. 11, we compare the achievable rates of the DFP policy for fully-correlated and independent (asynchronous) uniformly-distributed (i.e., not Bernoulli) energy arrivals with the support of $[0, B_k]$ at user k. We note that fully-correlated energy arrivals yield lower sum rates. However, the gap between the two is less than the gap between the performances of the fully-correlated and independent Bernoulli energy arrivals in Fig. 10. In Fig. 12, we show the long-term average rate regions obtained by the DFP policy for fully-correlated and independent energy arrivals for Bernoulli and uniform-distributed energy arrivals. We observe that in both cases, independent arrivals yield larger rates, and also uniform arrivals yield larger rates than Bernoulli arrivals.

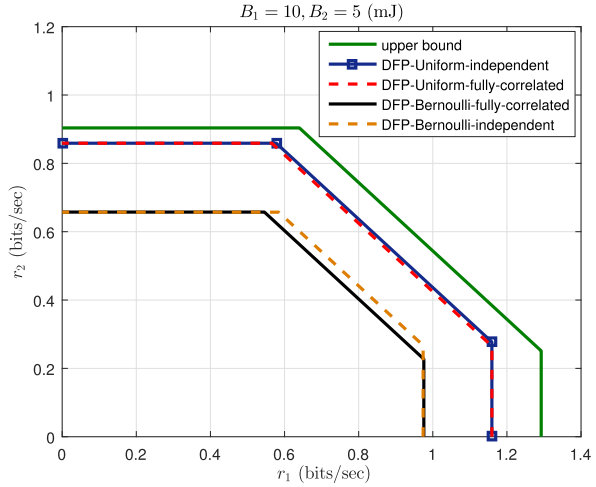

Fig. 12. Achievable rate regions (fully-correlated and independent arrivals for uniform and Bernoulli).

VII. Conclusion

We studied the optimal and near-optimal online power control policies which achieve the largest long-term average rate region for a two-user multiple access channel under equal average recharge rate per unit battery. We first considered the synchronous i.i.d. Bernoulli energy arrivals and obtained the exactly optimum policy. For this case, we showed that the long-term average rate region is a single pentagon and the optimal power allocation achieving the boundary of this region is decreasing between energy arrivals. The fractional form of the optimal policy and the single pentagon structure of the long-term average rate region motivated the proposed distributed fractional power (DFP) policy. The DFP policy is a function of the battery size and the average recharge rate. Each user knows only its own average recharge rate. We showed that under the DFP policy and for Bernoulli energy arrivals, synchronous arrivals yield a smaller long-term average rate region than the asynchronous arrivals. Then, we showed that under the DFP policy, Bernoulli energy arrivals yield a smaller long-term average rate region than general energy arrivals. We developed a lower bound for the synchronous Bernoulli energy arrivals and a universal upper bound for all energy arrivals and all online policies. We showed that the developed lower and upper bounds are within a constant gap of each

other, and hence, the optimal online policy is within a constant gap to the proposed DFP policy for equal normalized average recharge rates.

APPENDIX
PROOF OF THEOREM 3

As discussed at the beginning of Sub-section V.A, we consider a synchronous Bernoulli energy arrival process with parameter p, and an asynchronous Bernoulli energy arrival process with parameters p_{00}, p_{01}, p_{10} and p_{11} with $p_{01}=p_{10}$. As also discussed, it suffices to consider only the sum rate, i.e., we need to show,

$$\lim_{n\to\infty}\frac{1}{n}\mathbb{E}_{sync}\left[\sum_{i=1}^{n}\frac{1}{2}\log\left(1+pb_{1i}+pb_{2i}\right)\middle|x_1,x_2\right] \le \lim_{n\to\infty}\frac{1}{n}\mathbb{E}_{async}\left[\sum_{i=1}^{n}\frac{1}{2}\log\left(1+pb_{1i}+pb_{2i}\right)\middle|x_1,x_2\right] \quad (56)$$

where pb_{1i} and pb_{2i} inside the logarithms show that p fraction of the available energy b_{1i} and b_{2i} are being used for transmission, and x_k is the initial battery state at the kth user in slot 1. To prove (56), it suffices to prove it for each individual slot, i.e.,

$$\mathbb{E}_{sync}\left[\log\left(1+pb_{1i}+pb_{2i}\right)\middle|x_1,x_2\right] \le \mathbb{E}_{async}\left[\log\left(1+pb_{1i}+pb_{2i}\right)\middle|x_1,x_2\right], \quad \forall i \quad (57)$$

To give intuition, we first prove the inequality for a few indices. First note that when $i=1$, both sides of (57) are identical and equal to $\log(1+px_1+px_2)$, and therefore, the inequality in (57) holds as an equality.

For $i=2$, we evaluate the expectations by considering the possibilities of an energy arrival and no arrival in slot 1, for the synchronous case as,

$$\begin{aligned}\mathbb{E}_{sync}&\left[\log\left(1+pb_{12}+pb_{22}\right)\middle|x_1,x_2\right]\\ &= p\log\left(1+pB_1+pB_2\right)\\ &\quad+(1-p)\log\left(1+p(1-p)x_1+p(1-p)x_2\right) \quad (58)\end{aligned}$$

and for the asynchronous case as,

$$\begin{aligned}\mathbb{E}_{async}&\left[\log\left(1+pb_{12}+pb_{22}\right)\middle|x_1,x_2\right]\\ &= p_{11}\log\left(1+pB_1+pB_2\right)\\ &\quad+p_{10}\log\left(1+pB_1+p(1-p)x_2\right)\\ &\quad+p_{01}\log\left(1+p(1-p)x_1+pB_2\right)\\ &\quad+p_{00}\log\left(1+p(1-p)x_1+p(1-p)x_2\right) \quad (59)\\ &\ge p_{11}\log\left(1+pB_1+pB_2\right)\\ &\quad+p_{10}\log\left(1+p(1-p)x_1+p(1-p)x_2\right)\\ &\quad+p_{01}\log\left(1+pB_1+pB_2\right)\\ &\quad+p_{00}\log\left(1+p(1-p)x_1+p(1-p)x_2\right) \quad (60)\\ &= p\log\left(1+pB_1+pB_2\right)\\ &\quad+(1-p)\log\left(1+p(1-p)x_1+p(1-p)x_2\right) \quad (61)\\ &= \mathbb{E}_{sync}\left[\log\left(1+pb_{12}+pb_{22}\right)\middle|x_1,x_2\right] \quad (62)\end{aligned}$$

where the inequality in (60) follows from Lemma 3 and the fact that $p_{01}=p_{10}$; (61) follows because $p_{11}+p_{01}=p$ and $p_{00}+p_{10}=1-p$; and (62) follows from (58).

For $i=3$, we evaluate the expectations by considering the possibilities of energy arrivals and no arrivals in slots 1 and 2, for the synchronous case as,

$$\begin{aligned}\mathbb{E}_{sync}&\left[\log\left(1+pb_{13}+pb_{23}\right)\middle|x_1,x_2\right]\\ &= p\log\left(1+pB_1+pB_2\right)\\ &\quad+p(1-p)\log\left(1+p(1-p)B_1+p(1-p)B_2\right)\\ &\quad+(1-p)^2\log\left(1+p(1-p)^2x_1+p(1-p)^2x_2\right) \quad (63)\end{aligned}$$

and for the asynchronous case as,

$$\begin{aligned}\mathbb{E}_{async}&\left[\log\left(1+pb_{13}+pb_{23}\right)\middle|x_1,x_2\right]\\ &= p_{11}\log\left(1+pB_1+pB_2\right)\\ &\quad+p_{10}(1-p)\log\left(1+pB_1+p(1-p)^2\,x_2\right)\\ &\quad+p_{01}(1-p)\log\left(1+p(1-p)^2\,x_1+pB_2\right)\\ &\quad+p_{00}^2\log\left(1+p(1-p)^2\,x_1+p(1-p)^2\,x_2\right)\\ &\quad+p_{01}p_{00}\log\left(1+p(1-p)^2\,x_1+p(1-p)B_2\right)\\ &\quad+p_{10}p_{00}\log\left(1+p(1-p)B_1+p(1-p)^2\,x_2\right)\\ &\quad+p_{11}p_{00}\log\left(1+p(1-p)B_1+p(1-p)B_2\right)\\ &\quad+p_{01}p\log\left(1+p(1-p)B_1+pB_2\right)\\ &\quad+p_{10}p\log\left(1+pB_1+p(1-p)B_2\right) \quad (64)\\ &\ge p_{11}\log\left(1+pB_1+pB_2\right)\\ &\quad+p_{10}(1-p)\log\left(1+pB_1+pB_2\right)\\ &\quad+p_{01}(1-p)\log\left(1+p(1-p)^2\,x_1+p(1-p)^2\,x_2\right)\\ &\quad+p_{00}^2\log\left(1+p(1-p)^2\,x_1+p(1-p)^2\,x_2\right)\\ &\quad+p_{01}p_{00}\log\left(1+p(1-p)^2\,x_1+p(1-p)^2\,x_2\right)\\ &\quad+p_{10}p_{00}\log\left(1+p(1-p)B_1+p(1-p)B_2\right)\\ &\quad+p_{11}p_{00}\log\left(1+p(1-p)B_1+p(1-p)B_2\right)\\ &\quad+p_{01}p\log\left(1+p(1-p)B_1+p(1-p)B_2\right)\\ &\quad+p_{10}p\log\left(1+pB_1+pB_2\right) \quad (65)\\ &= p\log\left(1+pB_1+pB_2\right)\\ &\quad+p(1-p)\log\left(1+p(1-p)B_1+p(1-p)B_2\right)\\ &\quad+(1-p)^2\log\left(1+p(1-p)^2x_1+p(1-p)^2x_2\right) \quad (66)\\ &= \mathbb{E}_{sync}\left[\log\left(1+pb_{13}+pb_{23}\right)\middle|x_1,x_2\right] \quad (67)\end{aligned}$$

where (65) follows from Lemma 3 and the fact that $p_{01}=p_{10}$; (66) follows from adding up similar terms; and (67) follows from (63).

We now proceed to the proof of the general case where $i=k$. For this case, the sum rate for the synchronous

case is,

$$\mathbb{E}_{sync}\left[\log\left(1+pb_{1k}+pb_{2k}\right)\middle|x_1,x_2\right] = (1-p)^{k-1}\log\left(1+p(1-p)^{k-1}x_1+p(1-p)^{k-1}x_2\right) + \sum_{j=0}^{k-2} p(1-p)^j \log\left(1+p(1-p)^j B_1+p(1-p)^j B_2\right) \tag{68}$$

and for the asynchronous case is,

$$\begin{aligned}
&\mathbb{E}_{async}\left[\log\left(1+pb_{1k}+pb_{2k}\right)\middle|x_1,x_2\right] \\
&= p_{00}^{k-1}\log\left(1+p(1-p)^{k-1}x_1+p(1-p)^{k-1}x_2\right) \\
&+\sum_{j=0}^{k-2} p_{01}p_{00}^{j}(1-p)^{k-2-j}\log\left(1+p(1-p)^{k-1}x_1+p(1-p)^{j}B_2\right) \\
&+\sum_{j=0}^{k-2} p_{10}p_{00}^{j}(1-p)^{k-2-j}\log\left(1+p(1-p)^{j}B_1+p(1-p)^{k-1}x_2\right) \\
&+\sum_{j=0}^{k-3} p_{01}p_{00}^{j}p(1-p)^{k-3-j}\log\left(1+p(1-p)^{k-2}B_1+p(1-p)^{j}B_2\right) \\
&+\sum_{j=0}^{k-3} p_{10}p_{00}^{j}p(1-p)^{k-3-j}\log\left(1+p(1-p)^{j}B_1+p(1-p)^{k-2}B_2\right) \\
&+\sum_{j=0}^{k-4} p_{01}p_{00}^{j}p(1-p)^{k-4-j}\log\left(1+p(1-p)^{k-3}B_1+p(1-p)^{j}B_2\right) \\
&+\sum_{j=0}^{k-4} p_{10}p_{00}^{j}p(1-p)^{k-4-j}\log\left(1+p(1-p)^{j}B_1+p(1-p)^{k-3}B_2\right) \\
&\quad\vdots \\
&+\sum_{j=0}^{1} p_{01}p_{00}^{j}p(1-p)^{1-j}\log\left(1+p(1-p)^{2}B_1+p(1-p)^{j}B_2\right) \\
&+\sum_{j=0}^{1} p_{10}p_{00}^{j}p(1-p)^{1-j}\log\left(1+p(1-p)^{j}B_1+p(1-p)^{2}B_2\right) \\
&+p_{01}p\log\left(1+p(1-p)B_1+pB_2\right) \\
&+p_{10}p\log\left(1+pB_1+p(1-p)B_2\right) \\
&+\sum_{j=0}^{k-2} p_{11}p_{00}^{j}\log\left(1+p(1-p)^{j}B_1+p(1-p)^{j}B_2\right)
\end{aligned} \tag{69}$$

The proof for the general case follows similarly by applying Lemma 3 between all two consecutive terms except for the first and the last, and then, by adding up similar terms.

REFERENCES

[1] D. Gündüz, K. Stamatiou, N. Michelusi, and M. Zorzi, "Designing intelligent energy harvesting communication systems," *IEEE Commun. Mag.*, vol. 52, no. 1, pp. 210–216, Jan. 2014.

[2] S. Ulukus *et al.*, "Energy harvesting wireless communications: A review of recent advances," *IEEE J. Sel. Areas Commun.*, vol. 33, no. 3, pp. 360–381, Apr. 2015.

[3] J. Yang and S. Ulukus, "Optimal packet scheduling in an energy harvesting communication system," *IEEE Trans. Commun.*, vol. 60, no. 1, pp. 220–230, Jan. 2012.

[4] K. Tutuncuoglu and A. Yener, "Optimum transmission policies for battery limited energy harvesting nodes," *IEEE Trans. Wireless Commun.*, vol. 11, no. 3, pp. 1180–1189, Mar. 2012.

[5] O. Ozel, K. Tutuncuoglu, J. Yang, S. Ulukus, and A. Yener, "Transmission with energy harvesting nodes in fading wireless channels: Optimal policies," *IEEE J. Sel. Areas Commun.*, vol. 29, no. 8, pp. 1732–1743, Sep. 2011.

[6] C. K. Ho and R. Zhang, "Optimal energy allocation for wireless communications with energy harvesting constraints," *IEEE Trans. Signal Process.*, vol. 60, no. 9, pp. 4808–4818, Sep. 2012.

[7] J. Yang, O. Ozel, and S. Ulukus, "Broadcasting with an energy harvesting rechargeable transmitter," *IEEE Trans. Wireless Commun.*, vol. 11, no. 2, pp. 571–583, Feb. 2012.

[8] M. A. Antepli, E. Uysal-Biyikoglu, and H. Erkal, "Optimal packet scheduling on an energy harvesting broadcast link," *IEEE J. Sel. Areas Commun.*, vol. 29, no. 8, pp. 1721–1731, Sep. 2011.

[9] O. Ozel, J. Yang, and S. Ulukus, "Optimal broadcast scheduling for an energy harvesting rechargeable transmitter with a finite capacity battery," *IEEE Trans. Wireless Commun.*, vol. 11, no. 6, pp. 2193–2203, Jun. 2012.

[10] J. Yang and S. Ulukus, "Optimal packet scheduling in a multiple access channel with energy harvesting transmitters," *J. Commun. Netw.*, vol. 14, no. 2, pp. 140–150, 2012.

[11] Z. Wang, V. Aggarwal, and X. Wang, "Iterative dynamic water-filling for fading multiple-access channels with energy harvesting," *IEEE J. Sel. Areas Commun.*, vol. 33, no. 3, pp. 382–395, Mar. 2015.

[12] N. Su, O. Kaya, S. Ulukus, and M. Koca, "Cooperative multiple access under energy harvesting constraints," in *Proc. IEEE Globecom*, Dec. 2015, pp. 1–6.

[13] K. Tutuncuoglu and A. Yener, "Sum-rate optimal power policies for energy harvesting transmitters in an interference channel," *J. Commun. Netw.*, vol. 14, no. 2, pp. 151–161, 2012.

[14] C. Huang, R. Zhang, and S. Cui, "Throughput maximization for the Gaussian relay channel with energy harvesting constraints," *IEEE J. Sel. Areas Commun.*, vol. 31, no. 8, pp. 1469–1479, Aug. 2013.

[15] D. Gündüz and B. Devillers, "Two-hop communication with energy harvesting," in *Proc. IEEE CAMSAP*, Dec. 2011, pp. 201–204.

[16] Y. Luo, J. Zhang, and K. B. Letaief, "Optimal scheduling and power allocation for two-hop energy harvesting communication systems," *IEEE Trans. Wireless Commun.*, vol. 12, no. 9, pp. 4729–4741, Sep. 2013.

[17] B. Gurakan and S. Ulukus, "Energy harvesting diamond channel with energy cooperation," in *Proc. IEEE ISIT*, Jun./Jul. 2014, pp. 986–990.

[18] O. Orhan and E. Erkip, "Energy harvesting two-hop communication networks," *IEEE J. Sel. Areas Commun.*, vol. 33, no. 12, pp. 2658–2670, Dec. 2015.

[19] B. Devillers and D. Gündüz, "A general framework for the optimization of energy harvesting communication systems with battery imperfections," *J. Commun. Netw.*, vol. 14, no. 2, pp. 130–139, 2012.

[20] K. Tutuncuoglu, A. Yener, and S. Ulukus, "Optimum policies for an energy harvesting transmitter under energy storage losses," *IEEE J. Sel. Areas Commun.*, vol. 33, no. 3, pp. 476–481, Mar. 2015.

[21] J. Xu and R. Zhang, "Throughput optimal policies for energy harvesting wireless transmitters with non-ideal circuit power," *IEEE J. Sel. Areas Commun.*, vol. 32, no. 2, pp. 322–332, Feb. 2014.

[22] O. Orhan, D. Gündüz, and E. Erkip, "Energy harvesting broadband communication systems with processing energy cost," *IEEE Trans. Wireless Commun.*, vol. 13, no. 11, pp. 6095–6107, Nov. 2014.

[23] O. Ozel, K. Shahzad, and S. Ulukus, "Optimal energy allocation for energy harvesting transmitters with hybrid energy storage and processing cost," *IEEE Trans. Signal Process.*, vol. 62, no. 12, pp. 3232–3245, Jun. 2014.

[24] A. Arafa, A. Baknina, and S. Ulukus, "Energy harvesting two-way channels with decoding and processing costs," *IEEE Trans. Green Commun. Netw.*, vol. 1, no. 1, pp. 3–16, Mar. 2017.

[25] O. Ozel, S. Ulukus, and P. Grover, "Energy harvesting transmitters that heat up: Throughput maximization under temperature constraints," *IEEE Wireless Commun.*, vol. 15, no. 8, pp. 5440–5452, Aug. 2016.

[26] A. Baknina, O. Ozel, and S. Ulukus, "Energy harvesting communications under temperature constraints," in *Proc. Inf. Theory Appl. Workshop (ITA)*, Jan./Feb. 2016, pp. 1–10.

[27] K. Tutuncuoglu and A. Yener, "Communicating with energy harvesting transmitters and receivers," in *Proc. Inf. Theory Appl. Workshop (ITA)*, Feb. 2012, pp. 240–245.

[28] H. Mahdavi-Doost and R. D. Yates, "Energy harvesting receivers: Finite battery capacity," in *Proc. IEEE ISIT*, Jul. 2013, pp. 1799–1803.

[29] R. D. Yates and H. Mahdavi-Doost, "Energy harvesting receivers: Optimal sampling and decoding policies," in *Proc. IEEE GlobalSIP*, Dec. 2013, pp. 367–370.
[30] H. Mahdavi-Doost and R. D. Yates, "Fading channels in energy-harvesting receivers," in *Proc. CISS*, Mar. 2014, pp. 1–6.
[31] J. Rubio and A. Pascual-Iserte, "Energy-efficient resource allocation techniques for battery management with energy harvesting nodes: A theoretical approach," in *Proc. IEEE Wireless Commun. Netw. Conf. (WCNC)*, Apr. 2013, pp. 795–800.
[32] A. Arafa and S. Ulukus, "Optimal Policies for wireless networks with energy harvesting transmitters and receivers: Effects of decoding costs," *IEEE J. Sel. Areas Commun.*, vol. 33, no. 12, pp. 2611–2625, Dec. 2015.
[33] A. Arafa, A. Baknina, and S. Ulukus, "Energy harvesting two-way channel with decoding costs," in *Proc. IEEE ICC*, May 2016, pp. 1–6.
[34] B. Gurakan, O. Ozel, J. Yang, and S. Ulukus, "Energy cooperation in energy harvesting communications," *IEEE Trans. Commun.*, vol. 61, no. 12, pp. 4884–4898, Dec. 2013.
[35] K. Tutuncuoglu and A. Yener, "Energy harvesting networks with energy cooperation: Procrastinating policies," *IEEE Trans. Commun.*, vol. 63, no. 11, pp. 4525–4538, Nov. 2015.
[36] S. Mao, M. Cheung, and V. W. S. Wong, "An optimal energy allocation algorithm for energy harvesting wireless sensor networks," in *Proc. IEEE ICC*, Jun. 2012, pp. 265–270.
[37] V. Sharma, U. Mukherji, V. Joseph, and S. Gupta, "Optimal energy management policies for energy harvesting sensor nodes," *IEEE Trans. Wireless Commun.*, vol. 9, no. 4, pp. 1326–1336, Apr. 2010.
[38] R. Srivastava and C. E. Koksal, "Basic performance limits and tradeoffs in energy-harvesting sensor nodes with finite data and energy storage," *IEEE/ACM Trans. Netw.*, vol. 21, no. 4, pp. 1049–1062, Aug. 2013.
[39] M. B. Khuzani, H. E. Saffar, E. H. M. Alian, and P. Mitran, "On optimal online power policies for energy harvesting with finite-state Markov channels," in *Proc. IEEE ISIT*, Jul. 2013, pp. 1586–1590.
[40] Q. Wang and M. Liu, "When simplicity meets optimality: Efficient transmission power control with stochastic energy harvesting," in *Proc. IEEE INFOCOM*, Apr. 2013, pp. 580–584.
[41] N. Michelusi and M. Zorzi, "Optimal adaptive random multiaccess in energy harvesting wireless sensor networks," *IEEE Trans. Commun.*, vol. 63, no. 4, pp. 1355–1372, Apr. 2015.
[42] B. T. Bacinoglu and E. Uysal-Biyikoglu, "Finite horizon online lazy scheduling with energy harvesting transmitters over fading channels," in *Proc. IEEE ISIT*, Jun./Jul. 2014, pp. 1176–1180.
[43] B. T. Bacinoglu, E. Uysal-Biyikoglu, and C. E. Koksal. (2017). "Finite horizon energy-efficient scheduling with energy harvesting transmitters over fading channels." [Online]. Available: https://arxiv.org/abs/1702.06390
[44] D. Zhao, C. Huang, Y. Chen, F. Alsaadi, and S. Cui, "Resource allocation for multiple access channel with conferencing links and shared renewable energy sources," *IEEE J. Sel. Areas Commun.*, vol. 33, no. 3, pp. 423–437, Mar. 2015.
[45] R. Nagda, S. Satpathi, and R. Vaze, "Optimal offline and competitive online strategies for transmitter-receiver energy harvesting," in *Proc. IEEE ICC*, Jun. 2015, pp. 74–79.
[46] F. Amirnavaei and M. Dong, "Online power control optimization for wireless transmission with energy harvesting and storage," *IEEE Trans. Wireless Commun.*, vol. 15, no. 7, pp. 4888–4901, Jul. 2016.
[47] Z. Mao, C. E. Koksal, and N. B. Shroff, "Near optimal power and rate control of multi-hop sensor networks with energy replenishment: Basic limitations with finite energy and data storage," *IEEE Trans. Autom. Control*, vol. 57, no. 4, pp. 815–829, Aug. 2012.
[48] M. B. Khuzani and P. Mitran, "On online energy harvesting in multiple access communication systems," *IEEE Trans. Inf. Theory*, vol. 60, no. 3, pp. 1883–1898, Mar. 2014.
[49] D. Shaviv and A. Özgür, "Capacity of the AWGN channel with random battery recharges," in *Proc. IEEE ISIT*, Jun. 2015, pp. 136–140.
[50] D. Shaviv and A. Özgür, "Universally near optimal online power control for energy harvesting nodes," *IEEE J. Sel. Areas Commun.*, vol. 34, no. 12, pp. 3620–3631, Dec. 2016.
[51] A. Kazerouni and A. Özgür, "Optimal online strategies for an energy harvesting system with Bernoulli energy recharges," in *Proc. WiOpt*, May 2015, pp. 235–242.
[52] D. Shaviv, P.-M. Nguyen, and A. Özgür, "Capacity of the energy harvesting channel with a finite battery," in *Proc. IEEE ISIT*, Jun. 2015, pp. 131–135.
[53] A. Baknina and S. Ulukus, "Online scheduling for energy harvesting broadcast channels with finite battery," in *Proc. IEEE ISIT*, Jul. 2016, pp. 1984–1988.
[54] A. Baknina and S. Ulukus, "Optimal and near-optimal online strategies for energy harvesting broadcast channels," *IEEE J. Sel. Areas Commun.*, vol. 34, no. 12, pp. 3696–3708, Dec. 2016.
[55] A. Baknina and S. Ulukus, "Online policies for multiple access channel with common energy harvesting source," in *Proc. IEEE ISIT*, Jul. 2016, pp. 2739–2743.
[56] H. A. Inan and A. Özgür, "Online power control for the energy harvesting multiple access channel," in *Proc. WiOpt*, May 2016, pp. 1–6.
[57] T. M. Cover and J. A. Thomas, *Elements of Information Theory*. Hoboken, NJ, USA: Wiley, 2006.
[58] D. N. C. Tse and S. V. Hanly, "Multiaccess fading channels. I. Polymatroid structure, optimal resource allocation and throughput capacities," *IEEE Trans. Inf. Theory*, vol. 44, no. 7, pp. 2796–2815, Nov. 1998.
[59] A. Arapostathis, V. S. Borkar, E. Fernández-Gaucherand, M. K. Ghosh, and S. Marcus, "Discrete-time controlled Markov processes with average cost criterion: A survey," *SIAM J. Control Optim.*, vol. 31, no. 2, pp. 282–344, 1993.
[60] M. L. Puterman, *Markov Decision Processes: Discrete Stochastic Dynamic Programming*. Hoboken, NJ, USA: Wiley, 2014.
[61] D. P. Bertsekas, *Dynamic Programming and Optimal Control*, vol. 2, 3rd ed. Belmont, MA, USA: Athena Scientific, 2011.
[62] S. M. Ross, *Stochastic Processes*, vol. 2. New York, NY, USA: Wiley, 1996.
[63] S. P. Boyd and L. Vandenberghe, *Convex Optimization*. Cambridge, U.K.: Cambridge Univ. Press, 2004.
[64] A. W. Marshall, I. Olkin, and B. C. Arnold, *Inequalities: Theory of Majorization and Its Applications*, vol. 143. San Diego, CA, USA: Academic, 2016.

Abdulrahman Baknina (S'09) received the B.Sc. degree in electrical engineering and the M.Sc. degree in wireless communications from Alexandria University, Alexandria, Egypt, in 2010 and 2013, respectively. He is currently pursuing the Ph.D. degree with the Department of Electrical and Computer Engineering, University of Maryland, College Park, MD, USA. His research interests include optimization, information theory, and wireless communications.

Sennur Ulukus (S'90–M'98–SM'15–F'16) received the B.S. and M.S. degrees in electrical and electronics engineering from Bilkent University, and the Ph.D. degree in electrical and computer engineering from the Wireless Information Network Laboratory, Rutgers University. She was a Senior Technical Staff Member with the AT & T Laboratories-Research. She is currently a Professor of electrical and computer engineering with the University of Maryland, College Park, where she also holds a joint appointment with the Institute for Systems Research. Her research interests are in wireless communications, information theory, signal processing, and networks, with recent focus on information theoretic physical layer security, private information retrieval, energy harvesting communications, and wireless energy and information transfer.

Dr. Ulukus is a Distinguished Scholar-Teacher of the University of Maryland. She was a recipient of the 2003 IEEE Marconi Prize Paper Award in Wireless Communications, the 2005 NSF CAREER Award, the 2010–2011 ISR Outstanding Systems Engineering Faculty Award, and the 2012 ECE George Corcoran Education Award. She is currently an Area Editor for the IEEE TRANSACTIONS ON GREEN COMMUNICATIONS AND NETWORKING. She was an Editor for the IEEE JOURNAL ON SELECTED AREAS IN COMMUNICATIONS–Series on Green Communications and Networking from 2015 to 2016, the IEEE TRANSACTIONS ON INFORMATION THEORY from 2007 to 2010, and the IEEE TRANSACTIONS ON COMMUNICATIONS from 2003 to 2007. She was a Guest Editor for the IEEE JOURNAL ON SELECTED AREAS IN COMMUNICATIONS in 2015 and 2008, *Journal of Communications and Networks* in 2012, and the IEEE TRANSACTIONS ON INFORMATION THEORY in 2011. She is a General TPC Co-Chair of the 2017 IEEE ISIT, the 2016 IEEE GLOBECOM, the 2014 IEEE PIMRC, and the 2011 IEEE CTW.